Journal of Cleaner Production 116 (2016) 236–243

Contents lists available at ScienceDirect

Journal of Cleaner Production

journal homepage: www.elsevier.com/locate/jclepro

Investigating the possible usage of elephant grass ash to manufacture the eco-friendly binary cements

Erika Y. Nakanishi [a], Moisés Frías [b, *], Sérgio F. Santos [c], Michelle S. Rodrigues [a], Raquel Vigil de la Villa [d], Olga Rodriguez [b], Holmer Savastano Junior [a]

[a] University of São Paulo – FZEA – Department of Biosystems Engineering, Av. Duque de Caxias Norte, 225, 13635-900, Pirassununga, SP, Brazil
[b] Eduardo Torroja Institute (IETcc-CSIC), c/Serrano Galvache 4, 28033, Madrid, Spain
[c] São Paulo State University – Faculty of Engineering – Department of Materials and Technology, Guaratinguetá, SP, Brazil
[d] Geology and Geochemistry Department, Associate Unit CSIC-UAM, Autonomous University of Madrid, 28049, Madrid, Spain

ARTICLE INFO

Article history:
Received 23 January 2015
Received in revised form
30 November 2015
Accepted 31 December 2015
Available online 11 January 2016

Keywords:
Elephant grass ash
Pozzolanic activity
Blended cement
Hydrated phases
Properties

ABSTRACT

In recent years, agro-industrial residues are focusing attention worldwide as a new source of pozzolans; in Brazil one of the wastes generated from agro-industrial activities comes from elephant grass that is cultivated as biomass for energy cogeneration. The goal of this paper is to analyze the influence of elephant grass, once activated at 700 °C for 1 h in electric furnace, on the evolution of the hydration reaction as well as physical and mechanical properties in blended cement elaborated with 20% of elephant grass ash. For the present study, different instrumental techniques of characterization and methodologies (XRF, XRD, TG/DTG, mercury porosimetry, isothermal calorimetry and mechanical strength) were used. The results obtained in the present work show, that due to its high pozzolanic activity, the elephant grass ash activated at 700 °C can be used as an alternative pozzolan in the blended cement manufacture. Additions of 20% of ash confirm the formation of CSH gels and hexagonal C_4AH_{13} as main products from hydration as well as pozzolanic reaction. The 20% ash blended cement showed lower heat evolution than OPC and similar to the 20% silica fume blended cement, a 12% of reduction of compressive strength and an important reduction of pore sizes below 50 nm.

1. Introduction

Utilization of biomass ash from agro-industrial wastes in cement manufacturing can be an alternative solution to the incorporation of the traditionally used supplementary cementing materials (Demis et al., 2014; Villar-Cocina et al., 2013; Frías et al., 2012; Chiou and Chen, 2013; Sua-iam and Makul, 2013). It has been estimated that 18% replacement of cement result in a 17% reduction of CO_2 emissions (Ecosmart Concrete, 2008). In this sense, the agricultural industry plays an important role due to the high volume of waste produced (250 million of ton/year in Europe) (Barbieri et al., 2013), according to the FAO (OCDE-FAO, 2013), the world population will grow to 9 billion by 2050, implying an increase in food demand of 70% compared to today.

In Brazil, sugar cane is among the agricultural and agro-industrial sources, the most used as biomass for the production of clean energy and cheaper than produced from fossil combustibles (Frías et al., 2011). Besides this, there are other biomass sources with a more modest involvement in this type of energy such as the black liquor, wood waste, biogas, rice husk and eucalyptus (Rajamma et al., 2009; Sata et al., 2012; Cordeiro et al., 2009). However, recent new studies have being conducted in the search for new materials sources, such as the use of elephant grass (Strezov et al., 2008; Saidur et al., 2011; Xie et al., 2011) that has been traditionally cultivated mainly by animal producers in the past. The elephant grass presents relative growth rate (TCR) of 0.0083 g/g. day and cumulative production rate of 185 kg dry matter/ha/day. This type of biomass is also called “lignocellulosic biomass”, i.e, name given to species that besides serving for energy production and not compete with food crops (Abbasi and Abbasi, 2010). Brazil has the potential to produce 1.2 Gt of charcoal and a 2 Gt-average of bio-oils per year from elephant grass. In addition to the mentioned above, the elephant grass by their nature has other industrial applications such as: feed for animals, use in second generation of ethanol production and obtaining of charcoal

* Corresponding author. Tel.: +34 91 3020440.
E-mail address: mfrias@ietcc.csic.es (M. Frías).

http://dx.doi.org/10.1016/j.jclepro.2015.12.113
0959-6526/

(Menegol et al., 2014; Ajayi, 2011 Mesa-Pérez et al., 2014; Fontoura et al., 2015).

At this moment, there are some initiatives in Brazil for the application of elephant grass in co-generation processes (thermal-energy production). As an example, there is a recently launched power plant of co-generation (Sykué Bioenergia) located in São Desidério town, state of Bahia, Brazil, which operates with elephant grass as one of the biomass plantations available. This can be a clear indication of the scale-up potential for this technology. However, there is a lack of scientific-technical studies with blended-cement matrices carried out in laboratory, that are fundamental steps to give support to this technology transference to the industrial sector (full industrial scale application) (Nakanishi et al., 2014).

The ash resulting from burning (about 4–5% of the total mass), presents the suitable chemical, physical and mineralogical characteristics for its use as eco-efficient addition in the cement manufacture, and with the consequent economic, energy and environmental benefits. This follows from the fact that the pozzolanic material presents silica and alumina in its composition, which in presence of water reacts with the calcium hydroxide (CH) generated from the Portland cement hydration reaction, forming stable hydrated phases with cementing properties (ASTM Standard, 2012). Therefore, the use of active additions, besides reducing the content of the cement clinker and the associated generation of greenhouse gases (mainly CO_2), is expected to provide improvements in physical-technical properties of the resultant binder (Sata et al., 2012; Soriano et al., 2013; Cordeiro and Sales, 2014; Frías et al., 2013a, 2014, 2015; Sánchez de Rojas et al., 2006; Rodríguez et al., 2008; Medina et al., 2013, 2014).

Initials studies carried out by Nakanishi et al. (2014) in elephant grass ash-calcium hydroxide systems reported that this kind of ash showed high pozzolanic activity, which was comparable to that obtained with the commercial silica fume, standardized pozzolan well known for its activity in the short-term. The SEM/EDX analyses confirmed the presence of type II C–S–H gels with different morphologies (according to the Taylor's classification of Ca/Si ratio>1.5) (Taylor, 1997) as the unique hydrated phase produced during the pozzolanic reaction.

Despite the scientific advances achieved until now, and due to novelty of this research line, there are still significant scientific and technical gaps regarding the influence of this pozzolan in blended cement matrices. The main goal of the current work is to evaluate its influence on the kinetics of reaction, physical-technical properties and microporosity modifications in the corresponding blended cement pastes elaborated with 20% of elephant grass ash. The silica fume was used as the reference pozzolan.

2. Materials and methods

2.1. Materials

The elephant grass Cameroon variety (*Pennisetum purpureum*) (EGC), one of the two species grown in Brazil, used in this work was collected from the Pirassununga campus of the University of São Paulo (latitude 21°59′46″ S, longitude 47°25′33″ W, 627 m high above sea level). Once cut after 150 days of age, the whole plant was triturated and submitted to a drying process at 60 °C for 72 h. The ash was obtained by controlled burning process of 70 g of elephant grass in an electrical furnace with a 10 °C/min heating rate, first at 400 °C for 20 min, and then the same heating rate was applied until 700 °C and held constant for 60 min. The ash was submitted to a potassium extraction treatment using hydrochloric acid (HCl) solution (3% v/v) during 1 h at 90 °C (Lima et al., 2011), in order to reduce the K_2O content (from the starting content of 22% down to 8.6% by mass). The ash resulting from the extraction process (EGCA) was ground in a ceramic ball mill for 30 min, to homogenize the sample. Densified commercial silica fume (SF), Elkem M920D was used as reference.

The chemical composition of both pozzolans and OPC is shown in Table 1. From the chemical composition of the ash EGCA, one can notice that this present a different composition with respect to the other agro-industrial ashes, such as rice husk and sugar cane bagasse ashes. The content of silica (49.4%) for the EGCA is much lower than for the rice husk ash (85–90%) and slightly below the content presented by the sugar cane bagasse ash (59%), as well as showing higher contents of potassium and phosphate oxides (Frías and Sánchez de Rojas, 2013b). The mineralogical composition and also the fineness of the two ashes is depicted in Figs. 1 and 2 respectively. More detailed information can be found elsewhere (Nakanishi et al., 2014).

The Ordinary Portland cement (OPC) used was an initial high strength Portland cement (CP V-ARI) according to the Brazilian NBR 5733 standard (NBR-5733 Standard, 1991) equivalent to OPC Type I – ASTM C150. Applying the Bogue calculation (Taylor, 1997), the OPC is formed mineralogically by 62.92% of C_3S, 9.10% of C_2S, 4.67% of C_3A, and 9.18% of C_4AF. The specific surface area values obtained by means of the BET method for the three starting samples were of 1.38, 54.2 and 16.1 m^2/g respectively. Table 2 shows the identifications of the materials used in the present work.

2.2. Mixture proportions

The blended cement pastes were manufactured by partial replacement of OPC by 20% of each of the pozzolans (EGCA or SF) according to the existing Brazilian Standards (NBR-5763 standard, 1991).

The water/binder (w/b) ratio was equal to 0.5 for all the produced pastes. A 0.1% of superplasticizer (Melflux 2651 F) by mass of binder was used in all cases in order to improve the rheology of the pastes and helping with the molding process. Moreover, the higher fineness of pozzolans demands more water in the mixture, so in order to not make a change in the ratio w/b is advised the use of superplasticizer. The use of the superplasticizer was also important to avoid changes in the w/b ratio in the mixtures containing pozzolans with high fineness.

2.3. Chemical and physical characterization

The chemical characterization was carried out by the X-ray fluorescence (XRF), using the Advanced X-ray Axios spectrometer. The mineralogical composition was determined by X-ray diffraction (XRD), using the X Pert Pro equipment, with X Celerator detector.

The particle size distribution of the particles was determined by low angle scattering laser (Sympatec Helos 12LA). The test was conducted with the feed system in isopropyl alcohol as nonreactive liquid (Frías et al., 1991).

The thermogravimetric analyses (TG/DTA) of pastes were carried out with TA Instruments SDT Q600. The temperature range

Table 1
Chemical composition determined by XRF of OPC, EGCA and SF.

	SiO_2	Al_2O_3	Fe_2O_3	SO_3	MgO	P_2O_5	Cl	K_2O	CaO	LOI
	Oxides (% by mass)									
OPC	19.7	3.69	3.02	8.44	1.99	0.13	0.01	1.26	59.40	2.25
EGCA	49.4	0.47	0.83	0.47	4.22	9.91	0.46	8.60	10.4	14.6
SF	84.5	0.97	2.62	–	0.60	0.14	–	1.04	2.93	7.53

LOI = loss on ignition at 1000 °C.

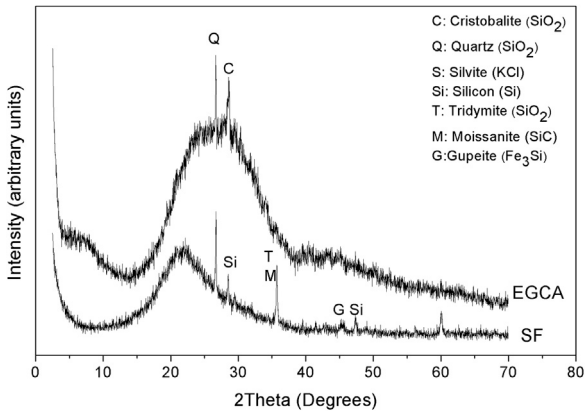

Fig. 1. XRD patterns of the treated cameroon ashes (EGC) and silica fume (SF).

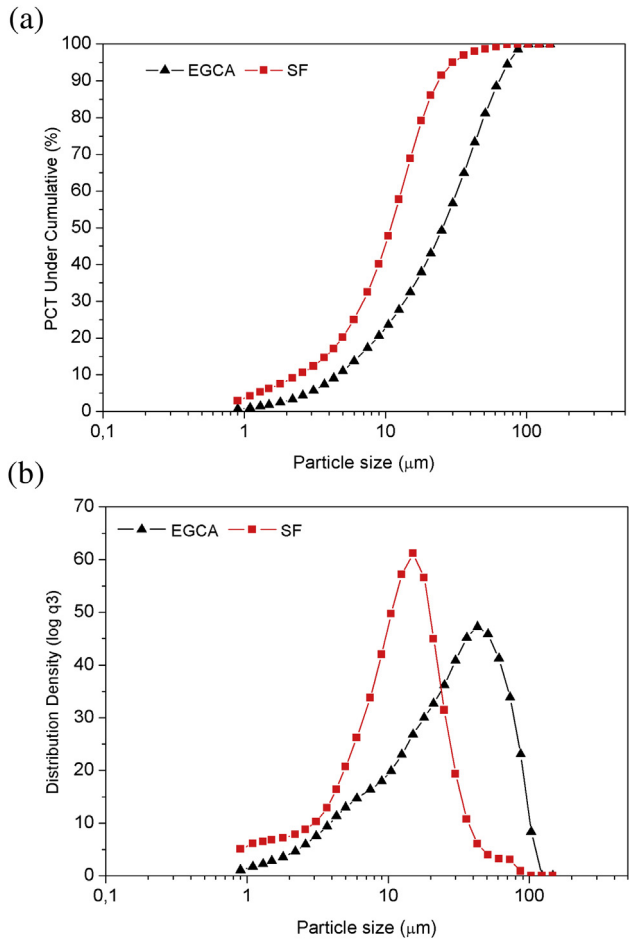

Fig. 2. Particle size distribution curves of the pozzolans before grinding: a) Cumulative, and b) Discrete distribution.

Table 2
Identification of the materials used in the experimental work.

Abbreviation	Complete name
EGC	Elephant Grass Cameroon
EGCA	Elephant Grass Cameroon ash
SF	Silica Fume
OPC	Ordinary Portland Cement

was 25–1000 °C, heating rate 10 °C/min and nitrogen atmosphere, and the sample size was about 30 mg.

The mineralogical composition of the bulk samples was determined by random powder X-ray diffraction (XRD) on a Siemens D-5000 (Munich, Germany) X-ray diffractometer fitted with a Cu anode. Their operating conditions were 30 mA and 40 kV and divergence of 2 and 0.6 mm with reception slits, respectively. The samples were scanned in (2y) 0.041 steps with a 3-scount time. The characterization and semi-quantification of bulk samples was carried out using the random power method operating from 3° to 65° 2θ at a rate of 2°/min. The semi-quantitative mineralogical composition was determined by the method of reflectant powers (Schultz, 1964). The areas under the reflection for each mineral were determined through Gaussian fitting where the base line intensity was subtracted by a conventional program (DRXWin). The percentage of error by this method is 10%.

The isothermal calorimetry study in the pastes was conducted for 3 days (72 h), in a Thermometric TAM-AIR calorimeter at 25 °C, using water as reference. The mixing of samples was performed manually by stirring the cement and water (binder/water ratio of 0.5). The measured data was the rate of heat, which after being normalized by the solid weight and calibrated, was expressed in J/h.g. The obtained value was then reported as the cumulative heat, which was the integral of the rate with time.

The determination of the specific surface area was performed with a Micromeritics ASAP 2000 by means of BET method (N_2 adsorption).

2.4. Text methods

In order to evaluate the compressive strength and the porosity of the blended pastes cylindrical specimens of 25 mm of diameter and 50 mm of height were prepared. The preparation of pastes was carried out according to Brazilian Standards NBR-7215 (1996). The samples were maintained in a curing room at 22 °C, with relative humidity of 80%, until 28, 60 and 90 days of hydration.

For the compressive test 10 specimens were used for each cement paste (OPC, OPC+20% EGCA, OPC+20% SF). The compressive test was conducted in saturated specimens with the universal testing machine EMIC, model DL-30000, equipped with a load cell of 50 kN, device displacement of 0.3 mm/min. Preliminary statistical analysis was initially performed through the Shapiro–Wilk test (normality) and Bartlett's test (homogeneity of treatments). An analysis of variance (ANOVA) was performed to assess whether there was an interaction between factors, paste type (OPC, OPC+20% EGCA, OPC+20% SF) and age assessment (28, 60 and 90 days). Moreover, these variables (paste type and age curing) were evaluated separately. Then a comparison between the mean values with the Tukey test at 5% significance level was performed.

The pore size distribution of the minicylinders was determined at 90 days of age. The equipment used was a Micromeritics 9320 Poresizer. Cubic samples of 10 mm were taken from central part of the minicylinders (25 mm diameter and 50 mm height) using a precision cutter Struers, model Miniton with the diamond cutting disc.

3. Results and discussion

3.1. Reaction kinetics of blended pastes

3.1.1. X-ray diffraction results

Fig. 3 shows the evolution of mineralogical phases by XRD with increasing hydration time. In the reference OPC cement, the following anhydrous phases were identified: alite (C_3S) in the reflection peaks to 5.90 Å (14.80°), 3.86 Å (22.96°), 3.51 Å (25.28°),

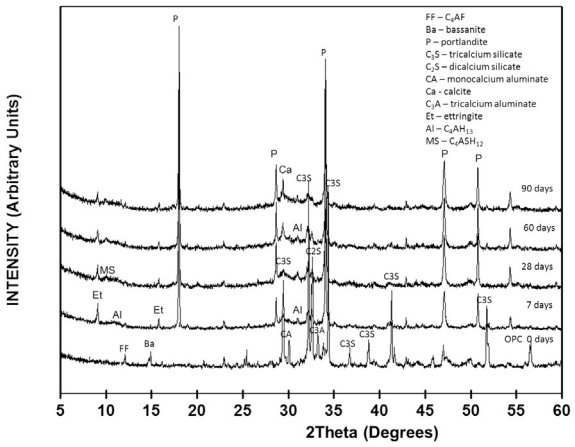

Fig. 3. X ray diffraction of the OPC paste at 0, 7, 28, 60 and 90 days.

3.34 Å (26.51°) and 3.22 Å (27.25°), belite (C_2S) at 2.75 Å (31.99°), 2.69 Å (12.76°), 2.19 Å (41.22°), 2.03 Å (44.69°) and 1.93 Å (45.70°), bassanite ($CaSO_4.1/2H_2O$) at 5.94 Å (14.72°), 3.45 Å (25.67°), 2.98 Å (29.69°), 2.78 Å (31.90°), 2.12 Å (42.25°) and 1.84 Å (49.36°), tricalcium aluminate (C_3A) at 2.71 Å (33.15°), 2.20 Å (40.91°), 1.92 Å (47.62°), and 1.89 Å (48.02°), mono-calcium aluminate (CA) at 2.98 Å (30.06°), 2.53 Å (35.59°) and 2.42 Å (37.28°), and ferritic phase (C_4AF) at 7.26 Å (12.19°), 3.64 Å (24.34°), 2.66 Å (33.87°), 2.64 Å (33.49°), 2.05 Å (44.11°) and 1.92 Å (47.09°).

At 7 days of hydration, the reflections corresponding to the bassanite and mono-calcium aluminate (CA) phases disappeared as crystalline phases; while with the progress of the hydration reaction (since 28 days), the anhydrous phases of OPC cement (C_3S, C_2S, C_3A and C_4AF) decreased in intensity, remaining traces from this age (Table 3).

As crystalline hydrated phases in OPC cement were identified by XRD, applying the reflectant power method: calcite with reflections at 3.86 (22.98°), 3.03 (29.09°), 2.49 (36.06°), 2.28 (39.34°) and 2.09 Å (43.19°), portlandite at 4.90 (18.05°), 2.62 (34.11°), 1.92 (47.13°), 1.79 (50.81°) and 1.68 Å (54.38°), ettringite at 9.73 Å (9.86°), 5.61 Å (15.72°), 3.88 Å (22.86°), 2.56 Å (34.91°) and 2.20 Å (40.74°), tetracalcium aluminate hydrate (C_4AH_{13}) at 7.9 Å (11.43°) and 2.88 Å (31.14°), and finally, mono sulfoaluminate hydrate ($C_4A\bar{S}H_{12}$) identified at 8.92 Å (9.92°) and 2.87 Å (31.15°).

Throughout a detailed observation of Table 3, the evolution of hydrated phases up to 90 days of reaction was observed. The portlandite was identified at all reaction ages with concentrations between 59% and 55%, detecting constant values between 60 and 90 days. Also, it is clearly observed the presence of ettringite at all reaction ages in almost constant concentration (16–10%) with a slight decrease with the increasing reaction time. $C_4A\bar{S}H_{12}$ phase was observed between 28 and 90 days in the concentration range of 7–4%. The formation of this phase corresponds to the partial decomposition of the ettringite. For the C_4AH_{13} phase a constant concentration was detected with very low values (around 4%) between 7 and 90 days; while calcite was observed at 28 days of reaction, whose value increases slightly with increasing curing time.

Despite low or null crystallinity of CSH gels, weak reflections were observed at 3.07 Å (28.96°), 2.80 Å (31.70°) and 1.83 Å (49.44°), which could not be semi-quantified.

The influence of elephant grass ash as pozzolan in the hydration reaction of 20% EGCA blended cement can be clearly seen in Table 4. The bassanite, C_3A and mono-calcium aluminate mineralogical phases showed the same trend as that observed for OPC cement at 7 days of curing. However, the addition of this kind of pozzolan (EGCA) showed an accelerating effect on the hydration of the C_3S and a retarding effect on the C_2S phase with respect to the hydration reaction of OPC cement. Hydrated phases observed in this binary cement system were the same as those mentioned for the OPC cement (Fig. 3). It is important to note that the addition of 20% EGCA favors the formation of the metastable C_4AH_{13} phase up to 90 days of reaction (Fig. 4). An increase in the content of portlandite was observed after 60 days of reaction, which may indicate the end of the pozzolanic reaction and the predominance of the hydration of OPC cement particles.

When carrying out a comparative study with 20% SF cement paste (Fig. 5 and Table 5) showed that the presence of SF in the cement paste promoted the partial conversion of ettringite to sulfoaluminate phase ($C_4A\bar{S}H_{12}$) from 7 days of curing. In all cases, calcite was identified as mineralogical phase from 60 days, mainly in cements made with SF. This fact would be directly related to the carbonation process of the portlandite during handling and storage of samples.

3.1.2. *Thermogravimetry analysis*

DTA curves of here cement pastes studied are shown in Figs. 6–8. The weight losses determined from TG data are shown in Table 5. In this table the chemical bonded water (determined from 60 to 350 °C) is included, as a measurement of hydration.

In all figures, 3 different zones can be observed:

a) From 60 to 350 °C, due to dehydration of main hydrated phases
b) About 450 °C, due to portlandite dehydroxilation
c) From 600 to 750 °C due to calcite decarbonation

The first signal (60–350 °C) involves the contribution of several overlapping peaks: loss of adsorbed and structural water of main hydrated phases formation during the hydration reaction. Taking into account the silica rich nature of EGCA and SF (Table 1), the

Table 3
Mineralogical composition of XRD of the OPC paste at 0, 7, 28, 60 and 90 days of curing.

% Mineral	0 days	7 days	28 days	60 days	90 days
C_4AF	4	4	4	3	2
Bassanite	9	–	–		–
C_3S	42	9	3	3	2
C_2S	25	4	4	4	3
CA	9	–	–	–	–
C_3A	11	4	4	3	–
Ettringite	–	16	13	10	10
$C_4A\bar{S}H_{12}$			7	4	4
$Ca(OH)_2$	–	59	52	55	55
C_4AH_{13}	–	4	4	4	4
$CaCO_3$	–	–	9	14	20

Table 4
Mineralogical composition of XRD of the OPC+20%EGCA paste at 0, 7, 28, 60 and 90 days of curing.

% Mineral	0 days	7 days	28 days	60 days	90 days
C_4AF	4	4	4	1	1
Bassanite	9	–	–		–
C_3S	42	7	5	2	–
C_2S	25	15	14	10	8
CA	9	–	–	–	–
C_3A	11	–	–	–	–
Ettringite	–	12	9	9	9
$C_4A\bar{S}H_{12}$			4	4	–
$Ca(OH)_2$	–	29	32	27	41
C_4AH_{13}	–	26	27	27	30
$CaCO_3$	–	7	5	20	11

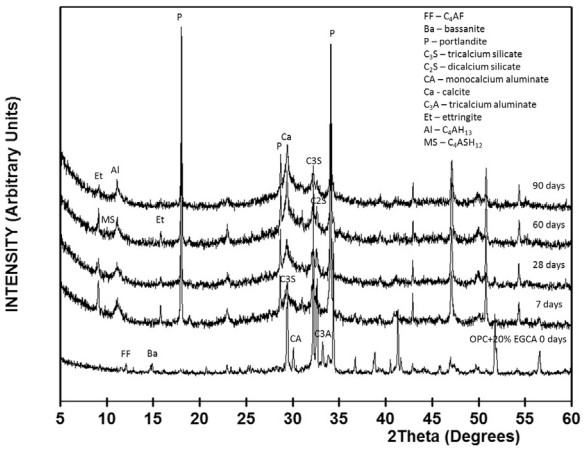

Fig. 4. X ray diffraction of the OPC+20%EGCA at 0, 7, 28, 60 and 90 days.

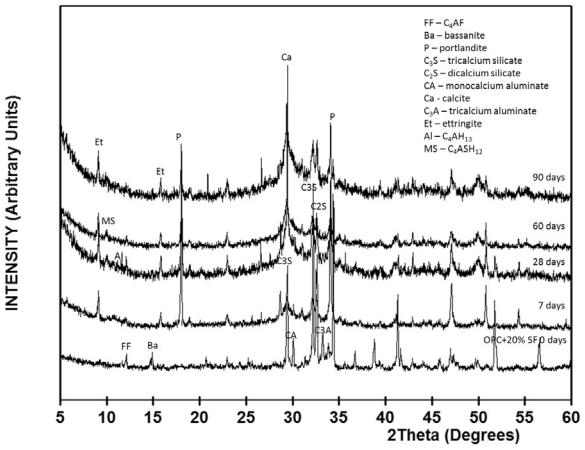

Fig. 5. X ray diffraction of the OPC+20%SF at 0, 7, 28, 60 and 90 days.

Table 5
Mineralogical composition of XRD of the OPC+20%SF paste at 0, 7, 28, 60 and 90 days of curing.

% Mineral	0 days	7 days	28 days	60 days	90 days
C_4AF	4	3	3	2	2
Bassanite	9	–	–		–
C_3S	42	2	2	–	–
C_2S	25	19	17	12	9
CA	9	–	–	–	–
C_3A	11	–	–	–	–
Ettringite	–	17	14	11	9
$C_4A\bar{S}H_{12}$			13	15	17
$Ca(OH)_2$	–	49	42	10	9
C_4AH_{13}	–	10	9	4	6
$CaCO_3$	–	–	–	46	48

band localized about 90–100 °C would correspond to the dehydroxilation of C–S–H gels. This affirmation is supported by previous works related to other agro-industrial ashes (bamboo, sugarcane and rice husk) and silica fume, which generated C–S–H gels as the main hydrated phase from pozzolanic reaction, with CaO/SiO_2 ratios below 1 (Jamil et al., 2013; Kar et al., 2012; Villar-Cociña et al., 2011; Frías et al., 2007; Sánchez de Rojas and Frías, 1996). This band is also due to ettringite decomposition, detected by XRD, but not by DTA analysis. The bands between 150 and 200 °C correspond to two dehydroxilation processes: monosulfoaluminate

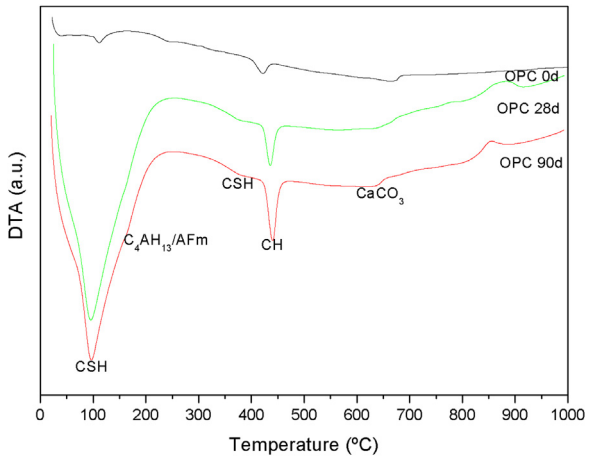

Fig. 6. DTA curves of OPC pastes at different ages of hydration.

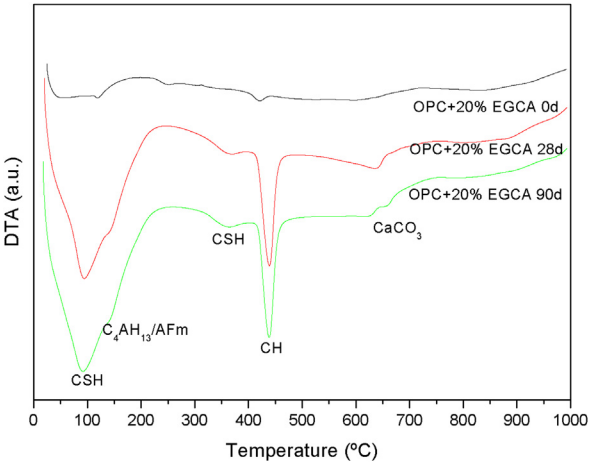

Fig. 7. DTA curves of OPC+20% SF pastes at different ages of hydration.

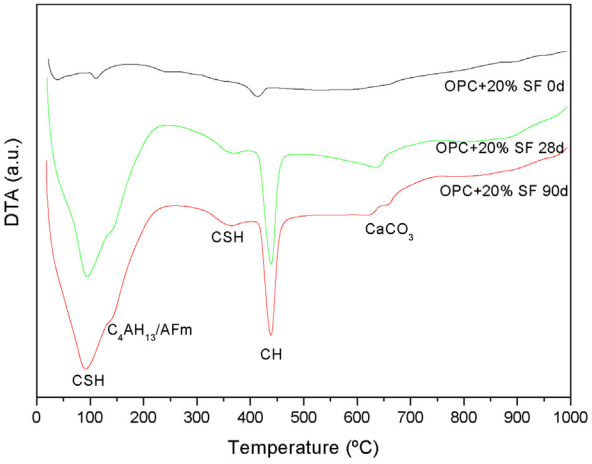

Fig. 8. DTA curves of OPC +20% EGCA pastes at different ages of hydration.

(AFm) and C_4AH_{13} phases. According to the XRD semi-quantitative analysis, this partially overlap band with the main band is located in 20% EGCA cements at 148 °C, moving to higher temperatures (160 °C) for 20% SF cements as a result of the C_4AH_{13}/AFm ratio (Taylor, 1997).

The bands situated between 250 and 370 °C can be also associated to C–S–H gels, increasing with curing time (Farmer et al., 1996). This band is better defined in EGCA pastes. The amount of chemically bonded water increased (Table 6), as expected, with hydration time, and is also higher for EGCA pastes at long hydration times (90 days). This data indicates that this waste shows higher pozzolanic activity than SF as previously reported by Nakanishi et al. (2014).

3.2. Isothermal calorimetry results

The calorimetry provides a continuous measure and consists a good method to study the initial phase of reaction where the rate of hydration heat is relatively high. According to Frías et al. (2000), the temperature of the blended cements can increase due to the high activity of pozzolanic materials such as metakaolin (MK) and may be higher as compared to the ordinary Portland cement paste, for the early age because of the double effect of exothermal hydration and pozzolanic reactions.

Isothermal calorimetry curves of pastes are presented in Fig. 9 with the heat flow *versus* time. In the first 30 min or pre-induction stage, it was observed higher heat flow of the OPC+20% SF than OPC+20%EGCA. In this initial stage the dissolution of the sulfates and calcium takes place, and the dissolution of the anhydrous phases (C_3S, C_3A, C_4AF) also starts. The consequence of these processes is the formation of a layer of calcium silicate hydrate (CSH) and a small amount of ettringite (AFt phase) (Quarcioni and Cincotto, 2006). In the induction period, between 1 and 6 h, the OPC paste shows a slight difference in the heat flow curve in comparison to the blended pastes.

During the acceleration period approximately between 6 h and 16 h, the process of dissolution and precipitation predominates. This period is characterized by a rapid formation of the CSH gels, as well as portlandite. The evolution of heat flow of blended cements was very similar, with no differences related to the nature of the pozzolan (EGCA or SF). In both cases, the heat flows were lower than for the OPC cement. These findings match with most of the pozzolan used in the manufacture of commercial cements, which are characterized by reducing the heat flow with respect to the reference cement matrix by its physical effect (dilution) at short term. As an exception to the mentioned above, silica fume for their chemical and physical characteristics tends to release more heat than OPC (Frías et al., 2000; Cheng-yi and Feldman, 1985). However, this fact is not observed in the present work.

This irregular behavior of the silica fume could be partially related to its low total silica content (84.5%) and low pozzolanic reaction rate as reported in a previous paper (Nakanishi et al., 2014). It could also be explained by the particle size distribution (Fig. 2). The higher the frequencies of distribution for silica fume is around 10 μm what can be an indication of poor dispersion of the individual particles, since the starting silica fume was densified.

The deceleration period, around 16 h–42 h, is characterized by the gradual decrease in the rate of heat evolution, since there is a reduction of ions in solution. This deceleration may be associated with the formation of ettringite (AFt phase) (Quarcioni, 2008).

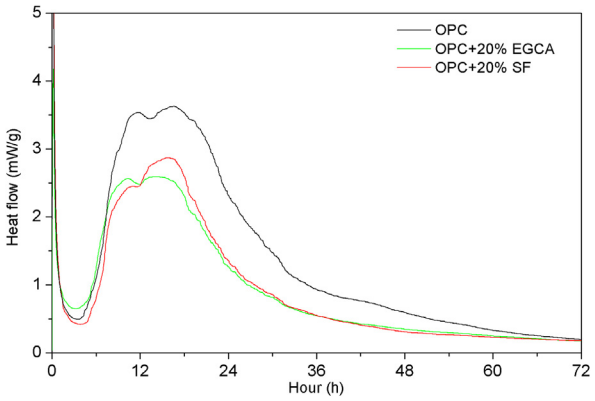

Fig. 9. Isothermal calorimetry curves for reference paste and pastes with 20% of pozzolanic addition.

There is a similarity of heat flow between the OPC+20% EGCA and OPC+20%SF. This similarity can be observed in the graph of Fig. 10, which shows the cumulative heat curves. The curves corresponding to OPC pastes showed a higher heat accumulation than others pastes. Thus, adding 20% EGCA or 20% SF, promotes a smaller heat release.

3.3. Mechanical behavior of the pastes by compressive strength

Table 7 shows the results of the multiple comparisons of the values of compressive strength of pastes by analysis of variance (ANOVA) and Tukey test. The pastes were evaluated at 28, 60 and 90 days of age. The ANOVA showed no statistically significant difference between the compressive strength values of the same paste for the curing ages.

The microstructure of hardened Portland cement paste and cement based materials is intrinsically unstable. The evolution of compressive strength of the paste at different ages, as verified with experimental data (Table 7), indicates complex hydration kinetics, taken into account that main constituents in Portland cement paste

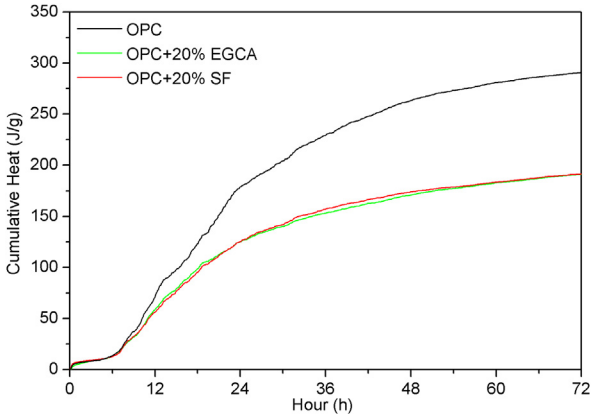

Fig. 10. Cumulative heat curves of the cementitious pastes.

Table 6
Weight losses of the pastes at different temperatures.

Temperature range (°C)	OPC			OPC+20% SF			OPC+20% EGCA		
	0 days	28 days	90 days	0 days	28 days	90 days	0 days	28 days	90 days
60–350	1.94	11.28	12.08	1.47	12.98	13.59	3.58	12.56	14.14
450–500	0.76	5.10	5.83	0.62	3.07	2.87	0.84	4.12	3.07
600–750	2.14	2.39	4.69	1.45	2.80	2.80	1.68	3.72	3.50

Table 7
Multiple comparisons of mean values of compressive strength (MPa) of pastes by Tukey test.

Pastes	Age (days of curing)		
	28	60	90
OPC	$37.0^{a\ DE}$	36.6^{aF}	34.1^{aH}
OPC+20%EGCA	31.0^{bD}	29.0^{bG}	28.0^{bH}
OPC+20%SF	40.0^{cE}	$32.0^{c\ FG}$	34.8^{cH}

Lower case letters are for comparison of values in the same line. Upper case letters are for comparison of values in the same column. The values with same letter in the line or columns do not differ by Tukey test ($p < 0.05$).

at the micro-scale, including CH and CSH gel. From 28 to 90 days of age the degree of hydration of the cement paste changes, as consequence appears different size of pores in the microstructure of the hardened cement paste covers a notable range from nanometric gel pores to micrometric capillary pores (Fig. 11) that interfere in the compressive strength of the pastes.

However, at 90 day of age, some stability is reached by pastes. It is observed that OPC+20%SF and OPC+20% EGCA show no statistical difference when compared to the OPC. Despite the additional time needed to OPC+20% EGCA for reaching the similar compressive strength of the OPC paste, these results indicate the potential of the elephant grass ash as pozzolanic mineral addition to partially replace Portland cement.

3.4. Microporosity of cement pastes

Reducing the volume of pores in a cementitious matrix is related to the evolution of pozzolanic activity and the formation of CSH,

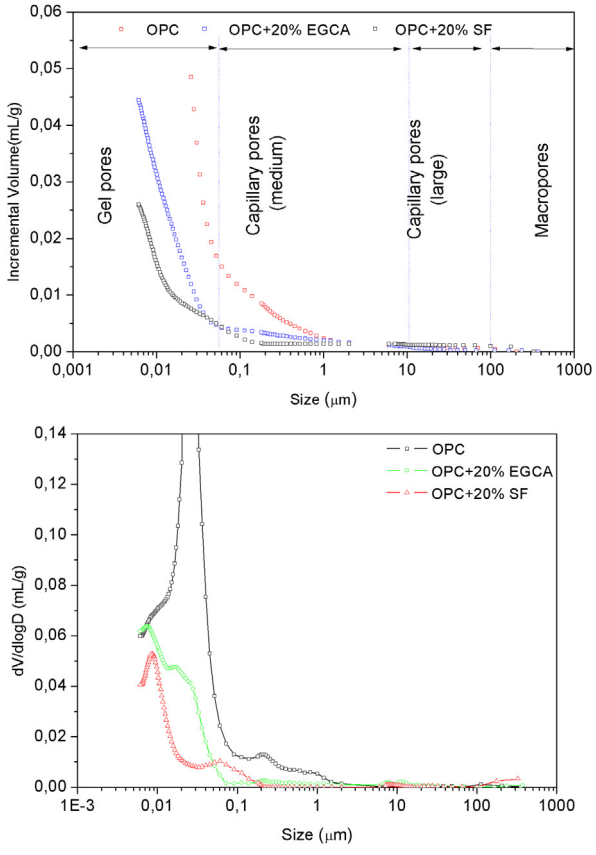

Fig. 11. Up) Evolution of pore sizes, Down) Distribution density of pore sizes at 90 days of age for the different cementitious pastes.

which strongly influences the increased strength of the matrix, as well as decreasing permeability and improving chemical durability (Metha, 1981). According to Mehta and Gjorv (1982), CSH formed by the pozzolanic reaction are less dense than the same product formed by hydrating a system with only Portland cement, and therefore has a smaller amount and matrix pore size. Fig. 11 shows the curves of the incremental volume (up) and distribution density (down) of the three cements versus pore sizes.

A detailed observation of Fig. 11 up indicates that the blended pastes (20% EGCA and 20% SF) cured at 90 days of hydration presented an important refining process of the pore sizes when compared to OPC paste. In both cases, the most of the sizes are below 0.05 μm, which corresponding to the gel pores, and a minimum proportion of capillary pores between 0.05 μm and 10 μm. It can be noted that the OPC+20% SF pastes had lower volume and capillary gel structure compared to the OPC+20% EGCA. The pore size density curves (Fig. 11 down) states clearly the refinement of the pore sizes with 20% additions with respect to the OPC paste. According to this figure, most of the pores are located between 0.08 and 0.09 μm in the case of OPC and between 0.008 and 0.009 μm for both blended cements. These results are in the same trend as other agro-industrial waste, where a 25% porosity was detected in 20% rice husk ash blended cement (Siddique, 2008).

In general, the use of pozzolans in cementitious matrices contributes to the mechanical strength development as a result of the combination of physical and chemical effects. The mechanical effects are associated with the packing effects resulting from the mixtures and depend on the particle size of the pozzolan. According to Mehta and Gjorv (1982), the packing of the particles and the formation of the CSH contribute to reduction of pores, which increases the mechanical strength of the material. These statements were not observed in pastes with 20% EGCA, which showed a lower compressive resistance than SF paste (Table 7). Other factors may be involved in the porosity and mechanical resistance, among others as: irregular morphologies, roughness and the presence of micropores in the EGCA ash particles, which may have interfered in the significantly lower compressive strength when compared to OPC+20%SF.

4. Conclusions

The conclusions drawn from the experimental results are as follows:

1. The Cameroon elephant grass ash activated at 700 °C is formed by SiO_2, CaO, P_2O_5, MgO and K_2O, whose sum of oxides exceeds 80% of the total. Crystobalite and quartz are the crystalline compounds present in the starting ash.
2. According to the results from XRD and TG/DTA analysis, CSH gels and tetracalcium aluminate hydrate (C_4AH_{13}) were the main reaction products in 20% EGCA blended cement pastes, and AFm phase was in minor proportion (<5%). The same reaction products were identified when the addition was silica fume (SF), but in different concentrations.
3. The addition of 20% EGCA to the cement paste substantially reduces the heat generated in the first 6 h of hydration with respect to the OPC paste. At 78 h a reduction of 34% was detected in both blended cements with respect to the OPC.
4. After 90 days of curing age, the 20% EGCA paste showed similar mechanical behavior when compared to control paste and 20% SF.
5. The incorporation of 20% EGCA affected to the microporosity of cement paste. A pore size refinement process was clearly observed with respect to the OPC paste, forming gels pores mainly below 50 nm at 90 days of reaction. Values also ratified

by the pore sizes density curves, passing from 9 nm for the 20% EGCA to 90 nm for the 20% SF blended pastes.

In summary, the use of elephant grass ash as a future eco-efficient pozzolan is a suitable source to get alternative cementing materials from agro-industrial wastes and with a direct influence on the socio-economic development of a country, especially in tropical areas where this plant is perfectly adapted. However, additional research is necessary to achieve a complete study of the cement matrix (durability, high percentages of substitution, ash from energy cogeneration industry, longer hydration times).

Acknowledgments

The authors would like to thank the FAPESP (Project: 2011/16842-5, 2010/16524-0 and 2009/17293-5) and to i-LINK program between CSIC and FAPESP (Project 2013/50790-8, i-Link0675-2013) for their financial support. The authors are also grateful to the Framework Agreement of Collaboration between IETcc/CSIC (Spain) and FZEA/USP (Brazil) (ref: 2013040043) and to CNPq (project #306386/2013-5).

References

Abbasi, T., Abbasi, S.A., 2010. Biomass energy and the environmental impacts associated with its production and utilization. Renew. Sust. Energy Rev. 14, 919–937.
Ajayi, F.T., 2011. Effects of feeding ensiled mixtures of elephant grass (Pennisetum purpureum) with three grain legume plants on digestibility and nitrogen balance of West African Dwarf goats. Livest. Sci. 142, 80–44.
ASTM, 2012. Standard Specification for Coal Fly Ash and Raw or Calcined Natural Pozzolan for Use in Concrete.
Barbieri, L., Andreola, F., Lancellotti, I., Taurino, R., 2013. Management of agricultural biomass wastes: preliminary study on characterization and valorisation in clay matrix bricks. Waste. Manage 33, 2307–2315.
Cheng-yi, H., Feldman, R.F., 1985. Hydration reactions in portland cement-silica fume blends. Cem. Concr. Res. 15, 585–592.
Chiou, I.J., Chen, C.H., 2013. Reuse of incinerated ash from industrial sludge-derived fuel. Constr. Build. Mater 49, 233–239.
Cordeiro, G.C., Sales, C.P., 2014. Pozzolanic activity of elephant grass ash and its influence on the mechanical properties of concrete. Cem. Concr. Compos 55, 331–336.
Cordeiro, G.C., Toledo Filho, R.D., Fairbairn, E.M.R., 2009. Effect of calcination temperature on the pozzolanic activity of sugar cane bagasse ash. Constr. Build. Mater 23, 3301–3303.
Demis, S., Tapali, J.G., Papadakis, V.G., 2014. An investigation of the effectiveness of the utilization of biomass ashes as pozzolanic materials. Constr. Build. Mater 68, 291–300.
Ecosmart Concrete, 2008. Environmental Impact-cement Production and the CO_2 Challenge. Ecosmart Foundation, Canada.
Farmer, V.C., Jeevartnam, J., Speakman, K., 1996. Thermal decomposition of 14 A tobermorite from crestmore. In: Rpt, U.S.H.R.B.S. (Ed.), Proc of Syrup Structure of Portland Cement Paste and Concrete, pp. 291–299.
Fontoura, C.F., Brandão, L.E., Gomes, L.L., 2015. Elephant grass biorefineries: towards a cleaner Brazilian energy matrix. J. Clean. Prod. 96, 85–93.
Frías, M., Sánchez de Rojas, M.I., 2013b. Artificial pozzolans in eco-efficient. In: Pacheco-Togal, F., Jalali, S., Labrincha, J., John, V.M. (Eds.), Eco-efficient Concrete. Woodhead Publishing Limited, Cambridge, pp. 105–122.
Frias, M., Sánchez de Rojas, M.I., Luxan, M.P., Garcia, N., 1991. Determination of specific surface-area by the laser diffraction technique – comparison with the Blaine permeability method. Cem. Concr. Res. 21, 709–717.
Frias, M., Sánchez de Rojas, M.I., Cabrera, J., 2000. The effect that the pozzolanic reaction of metakaolin has on the heat evolution in metakaolin-cement mortars. Cem. Concr. Res. 30, 209–216.
Frías, M., Villar-Cociña, E., Valencia-Morales, E., 2007. Characterisation of sugar cane straw waste as pozzolanic material for construction: calcining temperature and kinetic parameters. Waste Manag. 27, 533–538.
Frías, M., Villar, E., Savastano, H., 2011. Brazilian sugar cane bagasse ashes from the cogeneration industry as active pozzolans for cement manufacture. Cem. Concr. Compos 33, 490–496.
Frías, M., Savastano, H., Villar, E., Sánchez de Rojas, M.I., Santos, S., 2012. Characterization and properties of blended cement matrices containing activated bamboo leaf wastes. Cem. Concr. Compos 34, 1019–1023.
Frías, M., Goñi, S., García, R., Vigil de la Villa, R., 2013a. Seawater effect on durability of ternary cements. Synergy of chloride and sulphate ions. Compos. Part B-Eng 46, 173–178.
Frías, M., Vigil de la Villa, R., de Soto, I., García, R., Baloa, T.A., 2014. Influence of activated drinking-water treatment waste on binary cement-based composite behavior: characterization and properties. Compos. Part B-Eng 60, 14–20.
Frías, M., Rodríguez, O., Sánchez de Rojas, M.I., 2015. Paper sludge, an environmentally sound alternative source of MK-based cementitious materials. A review. Constr. Build. Mater 74, 37–48.
Jamil, M., Kaish, A.B., Raman, S.N., Zain, M.F.M., 2013. Pozzolanic contribution of rice husk ash in cementitious system. Constr. Build. Mater 47, 588–593.
Kar, A., Ray, I., Unnikrishnan, A., Davalos, J.F., 2012. Estimation of C–S-H and calcium hydroxide for cement pastes containing slag and silica fume. Constr. Build. Mater 30, 505–515.
Lima, S.P.B., Vasconcelos, R.P., Paiva, O.A., Cordeiro, G.C., Chaves, M.R., Toledo Filho, R.D., 2011. Production of silica gel from residual rice husk ash. Quím. Nova 34, 71–75.
Medina, C., Sánchez de Rojas, M.I., Frías, M., 2013. Freeze-thaw durability of recycled concrete containing ceramic aggregate. J. Clean. Prod. 40, 151–160.
Medina, C., Zhu, W., Howind, T., Sánchez de Rojas, M.I., Frías, M., 2014. Influence of mixed recycled aggregate on the physical-mechanical properties of recycled concrete. J. Clean. Prod. 68, 216–225.
Mehta, P.K., 1981. Studies on blended Portland cements containing Santorin Earth. Cem. Concr. Res. 11, 507–518.
Mehta, P.K., Gjorv, O.E., 1982. Properties of Portland-cement concrete containing fly-ash and condensed silica-fume. Cem. Concr. Res. 12, 587–595.
Menegol, D., Luisi, A., Claudete, R., Pinheiro, A.J., Camassola, M., 2014. Potential of a Penicillium echinulatum enzymatic complex produced in either submerged or solid-state cultures for enzymatic hydrolysis of elephant grass. Fuel 133, 232–240.
Mesa-Pérez, J.M., Cortez, L.A.B., Marín-Mesa, H.R., Rocha, J.D., Peláez-Samaniego, M.R., Cascarosa, E., 2014. A statistical analysis of the auto thermal fast pyrolysis of elephant grass in fluidized bed reactor based on produced charcoal. Appl. Therm. Eng. 65, 322–329.
Nakanishi, E.Y., Frías, M., Martínez-Ramírez, S., Santos, S.F., Rodrigues, M.S., Rodríguez, O., Holmer, S., 2014. Characterization and properties of elephant grass ashes as supplementary cementing material in pozzolan/Ca(OH)2 pastes. Constr. Build. Mater 73, 391–398.
NBR-5733, 1991. Cimento Portland de alta resistência inicial.
NBR-5763, 1991. Cimento Portland Puzolânico.
NBR-7215, 1996. Cimento Portland – Determinação da resistência à compressão.
OCDE/FAO, 2013. In: Chapingo, U.A. (Ed.), OCDE-FAO Agricultural Perspectives 2013-2022. Texcoco, Estado de México (in spanish).
Quarcioni, V.A., 2008. Influence of Hydrated Lime on Initial Stage of Hydration of Portland Cement – Paste Study. Polytechnic School of the University of São Paulo.
Quarcioni, V.A., Cincotto, M.A., 2006. Optmization of calculation method for determination of composition of hardened mortars of Portland cement and hydrated lime made in laboratory. Constr. Build. Mater 20, 1069–1078.
Rajamma, R., Ball, R.J., Tarelho, L.A.C., Allen, G.C., Labrincha, J.A., Ferreira, V.M., 2009. Characterisation and use of biomass fly ash in cement-based materials. J. Hazard. Mater 172, 1049–1060.
Rodriguez, O., Frias, M., Sanchez de Rojas, M.I., 2008. Influence of the calcined paper sludge on the development of hydration heat in blended cement mortars. J. Therm. Anal. Calorim. 92, 865–871.
Saidur, R., Abdelaziz, E.A., Demirbas, A., Hossain, M.S., Mekhilef, S., 2011. A review on biomass as a fuel for boilers. Renew. Sust. Energy Rev. 15, 2262–2289.
Sánchez de Rojas, M.I., Frías, M., 1996. The pozzolanic activity of different materials, its influence on the hydration heat in mortars. Cem. Concr. Res. 26, 203–213.
Sánchez de Rojas, M.I., Marín, F., Rivera, J., Frías, M., 2006. Morphology and properties in blended cements with ceramic wastes as a pozzolanic material. J. Am. Ceram. Soc. 89, 3701–3705.
Sata, V., Tangpagasit, J., Jaturapitakkul, C., Chindaprasirt, P., 2012. Effect of W/B ratios on pozzolanic reaction of biomass ashes in Portland cement matrix. Cem. Concr. Compos 34, 94–100.
Schultz, L.G., 1964. Quantitative interpretation of the mineralogical composition from X-ray and chemical data for the Pierre Shale. Geol. Surv. Prof. Pap. 391-C, C1-C36.
Siddique, R., 2008. Waste Materials and By-products in Concrete. Springer, Berlin.
Soriano, L., Monzó, J., Bonilla, M., Tashima, M.M., Payá, J., Borrachero, M.V., 2013. Effect of pozzolans on the hydration process of Portland cement cured at low temperatures. Cem. Concr. Compos 42, 41–48.
Strezov, V., Evans, T.J., Hayman, C., 2008. Thermal conversion of elephant grass (Pennisetum Purpureum Schum) to bio-gas, bio-oil and charcoal. J. Bioresour. Techol. 99, 8394–8399.
Sua-iam, G., Makul, N., 2013. Use of increasing amounts of bagasse ash waste to produce self-compacting concrete by adding limestone powder waste. J. Clean. Prod. 57, 308–319.
Taylor, H.F.W., 1997. Cement Chemistry, second ed. Thomas Telford Services Ltd, London.
Villar-Cociña, E., Morales, E.V., Santos, S.F., Savastano, H., Frías, M., 2011. Pozzolanic behavior of bamboo leaf ash: characterization and determination of the kinetic parameters. Cem. Concr. Compos 33, 68–73.
Villar-Cocina, E., Frías, M., Hernandez-Ruiz, J., Savastano, H., 2013. Pozzolanic behaviour of a bagasse ash from the boiler of a Cuban sugar factory. Adv. Cem. Res. 25, 136–142.
Xie, X.-M., Zhang, X.Q., Dong, Z.X., Guo, H.R., 2011. Dynamic changes of lignin contents of MT- elephant grass and its closely related cultivars. J. Biomass Bioenerg 35, 1732–1738.